AN OVERVIEW OF SATURN NARROWBAND RADIO EMISSIONS OBSERVED BY CASSINI RPWS

S.–Y. Ye*, G. Fischer†, J. D. Menietti*, Z. Wang*,
D. A. Gurnett*, and W. S. Kurth*

Abstract

Saturn narrowband (NB) radio emissions are detected between 3 and 70 kHz, with occurrence probability and wave intensity peaking around 5 kHz and 20 kHz. The emissions usually occur periodically for several days after intensification of Saturn kilometric radiation (SKR). Originally detected by the Voyagers, the extended duration of the Cassini mission and the improved capabilities of the Radio and Plasma Wave Science (RPWS) instrument have significantly advanced our knowledge about them. For example, RPWS measurements of the magnetic component have validated the electromagnetic nature of Saturn NB emissions. Evidences show that the 20 kHz NB emissions are generated by mode conversion of electrostatic upper hybrid waves on the boundary of the plasma torus, whereas direction–finding results point to a source in the auroral zone for the 5 kHz component. Similar to SKR, the 5 kHz NB emissions have a clock–like modulation and display two distinct modulation periods identical to the northern and southern hemisphere periods of SKR. Polarization measurements confirm that most NB emissions are propagating in the L–O mode, with the exception of second harmonic NB emissions. At high latitudes closer to the planet, RPWS detected right hand polarized Z–mode NB emissions below the local electron cyclotron frequency (f_{ce}), which are believed to be the source of the L–O mode NB emissions detected above the local f_{ce}. Although the energy source for the generation of the Z–mode waves is still unclear, linear growth rate calculations indicate that the observed plasma distributions are unstable to the growth of electrostatic cyclotron harmonic emission. Alternatively, electromagnetic Z–mode might be directly generated by the cyclotron maser instability. The source Z–mode waves, upon reflection, propagate to the opposite hemisphere before escaping through mode conversion, which could explain the fact that both rotational modulation periods of NB emissions are observable in each hemisphere.

* *Department of Physics and Astronomy, University of Iowa, Iowa City, IA 52242, USA*
† *Space Research Institute, Austrian Academy of Sciences, Schmiedlstrasse 6, A-8042 Graz, Austria*

1 Introduction

Saturn narrowband emissions were first detected around 5 kHz during the Voyager 1 flyby of Saturn [Gurnett et al., 1981a]. The Voyager 1 Plasma Wave Science (PWS) instrument observation of a persistent 5 kHz narrowband emission over a 3–day period, during which Voyager 1 traveled from 3.26 R_S(Saturn radii) to 58.3 R_S, provided the best evidence that the 5 kHz narrowband emission is a freely propagating electromagnetic wave. Observations near the plasma torus showed that the narrowband emissions are observed only in the low–density regions outside of the torus where the wave frequency is greater than the local electron plasma frequency (f_{pe}), and that there was no obvious propagation effect at the local electron cyclotron frequency (f_{ce}). The lower cutoff at f_{pe} led to the conclusion that the narrowband emission was propagating in the L–O mode, although Voyager PWS used only one dipole antenna, hence no direct polarization measurement was available. Examination of Voyager 1 spectrograms during the Saturn flyby also revealed a periodic modulation of the narrowband emission intensities at the rotation period of Saturn [Gurnett et al., 1981a; Scarf et al., 1982].

Since 2004, the Radio and Plasma Wave Science (RPWS) instrument onboard Cassini revealed more interesting features of Saturn narrowband emissions. First of all, a new component of Saturn narrowband emissions was detected at higher frequencies (10 to 70 kHz). These emissions, referred to as 20–kHz narrowband emissions by Ye et al. [2009] and as n–SKR by Lamy et al. [2008], were not observed by Voyager 1 or 2 probably due to its lower intensity compared to the 5–kHz narrowband emission. Second, it is found that narrowband emissions are not only polarized as left hand ordinary (L–O) mode but sometimes also polarized as right hand extraordinary (R–X) mode. Third, the variety of Cassini orbits allowed the deduction of beaming and spatial distribution of narrowband emissions. Last but not the least, the long duration of the Cassini mission makes the determination of the rotational modulation type and the period of narrowband emissions possible. In this article, we will summarize the Cassini RPWS findings on Saturn narrowband emissions, primarily from Ye et al. [2010a] and Ye et al. [2010b].

2 Source Mechanism

Based on the similarities between the terrestrial continuum radiation and Saturn narrowband emissions, Gurnett et al. [1981a] proposed that Saturn narrowband emissions are mode converted from electrostatic upper hybrid waves excited near the boundary of the plasma torus via either a linear [Jones, 1976] or a non–linear mechanism [Melrose, 1981]. The mode conversion mechanism requires that intense electrostatic upper hybrid waves are excited when the local upper hybrid frequency $f_{UH} = \sqrt{f_{pe}^2 + f_{ce}^2}$ is close to the odd half harmonics of the local electron cyclotron frequency (f_{ce}) [Ashour–Abdalla and Kennel, 1978; Rönnmark, 1978]. Ye et al. [2009] modeled the source location of narrowband emissions by calculating the locations where the matching condition $f_{UH} \cong (n + 1/2)f_{ce}$ is met in a meridian plane (their Figure 1). The predicted source locations for the 5 and 20 kHz narrowband emissions are near their respective f_{pe} contour lines.

Ye et al. [2009] reported many cases in which Cassini went through the source region of the 20 kHz narrowband emissions, as indicated by a strong electrostatic wave immediately preceding or following the radio emission. Ye et al. [2009] show that Cassini was very close to the modeled source locations of narrowband emissions during the source crossing events, in which electromagnetic emissions are radiated from intense electrostatic upper hybrid waves. A list of narrowband source encounter events from Saturn orbit insertion (SOI) to mid 2008 can be found in Table 2 of Ye et al. [2009].

A wave growth analysis based on the electron distribution function measured near a possible source region indicated that electromagnetic Z–mode waves could be excited by cyclotron maser instability when the local upper hybrid frequency is close to the harmonics of the local electron cyclotron frequency, i.e. $f_{UH} \cong nf_{ce}$ [Menietti et al., 2009; Menietti et al., 2010]. These Z–mode waves can then mode convert to L–O mode on a density gradient or density irregularities. The fact that no intense electrostatic upper hybrid waves have been observed around the predicted source locations for 5 kHz narrowband emissions seems to suggest that the 5 kHz component is first generated as Z–mode wave and then mode converted to L–O mode.

3 Polarization and Intensity Measurements

3.1 Polarization of Saturn Narrowband Emissions

When narrowband emissions are observed at high latitudes, we assume that the radio emission propagates in free space mode right after it leaves the source region and its polarization with respect to the wave vector $\mathbf{k}$ then remains the same in the absence of plasma effects [Gurnett et al., 1988]. So the mode of propagation at the source can be determined based on the polarization measurement at the spacecraft and the knowledge of the source location.

Figure 1 shows apparent Poynting flux and apparent circular polarization spectrograms covering a 4 hour time span on DOY 092, 2007. For a description of direction finding and polarization measurement capabilities of Cassini RPWS, see Gurnett et al. [2004] and Cecconi and Zarka [2005]. The apparent polarization is defined in Fischer et al. [2009] and discussed in Ye et al. [2010a]. Note that the circular polarization sense of the narrowband emissions (at lower frequencies) are generally opposite to that of SKR, which is known to be emitted mostly in the R–X mode.

Figure 2 illustrates the geometry when Cassini detects both SKR and narrowband radio emissions at high northern latitudes. Because the beaming angle is smaller than $90°(\mathbf{k}\cdot\mathbf{B} > 0)$ for both SKR and narrowband emission in this situation, the real polarization sense of these two emissions should be like the mode of propagation at the source. However, in the case shown in Figure 1, the SKR source is on the side of the antenna plane (formed by the two electric antenna used in the measurement mode) where the sense of real polarization is opposite to the sense of apparent polarization. This means that an L–O mode emission appears to be right hand polarized (blue color) at the spacecraft, although its real sense

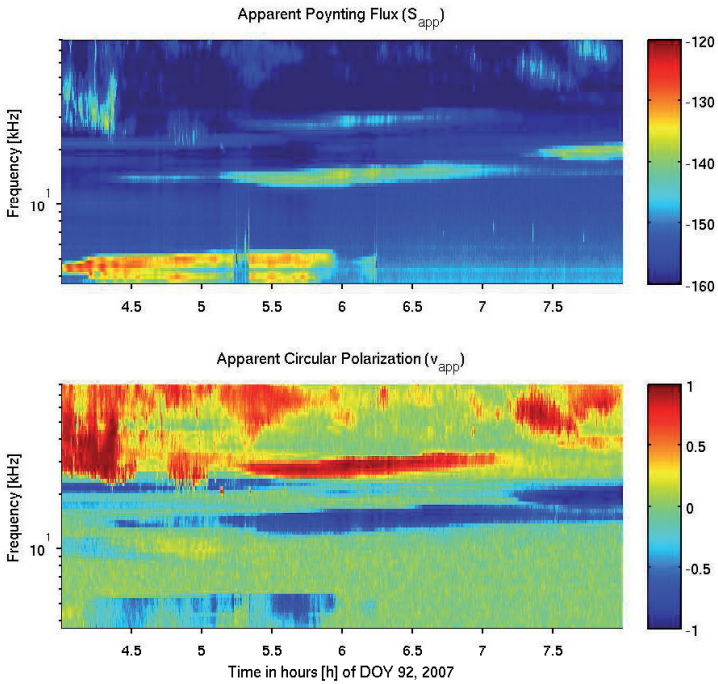

Figure 1: Narrowband emission with oppositely polarized second harmonic emission detected by Cassini/RPWS on DOY 092, 2007. The apparent Poynting flux S_{app} and the apparent circular polarization v_{app} are shown in the top and bottom, respectively. Cassini was located around 45° northern latitude, and the sense of real polarization is opposite to the sense of apparent polarization here.

is left hand. The R–X mode emission appears left hand polarized (red color), but its real sense is right hand.

Figure 1 also shows a pair of 20–kHz narrowband emissions that are observed simultaneously, with the top band near twice the frequency of the bottom band. The apparent circular polarization spectrogram (bottom panel) shows that the top band is polarized in the same sense as SKR. The intensities (top panel) of the top and bottom bands are observed to vary coherently. Goniopolarimetric results show that the top and bottom bands have nearly identical directions of arrival, ruling out the possibility that the beaming angle crossing 90° may have caused the polarization change. Therefore, the top band should be emitted in the R–X mode. Ye et al. [2009] proposed that these emissions are R–X mode emissions generated at second harmonic frequencies of the fundamental L–O mode emissions via a non–linear mode conversion process. Similar phenomena have been observed at Earth and discussed by James et al. [1974], Roux and Pellat [1979], Melrose [1991], and Willes et al. [1998]. If non–linear mode conversion applies to narrowband

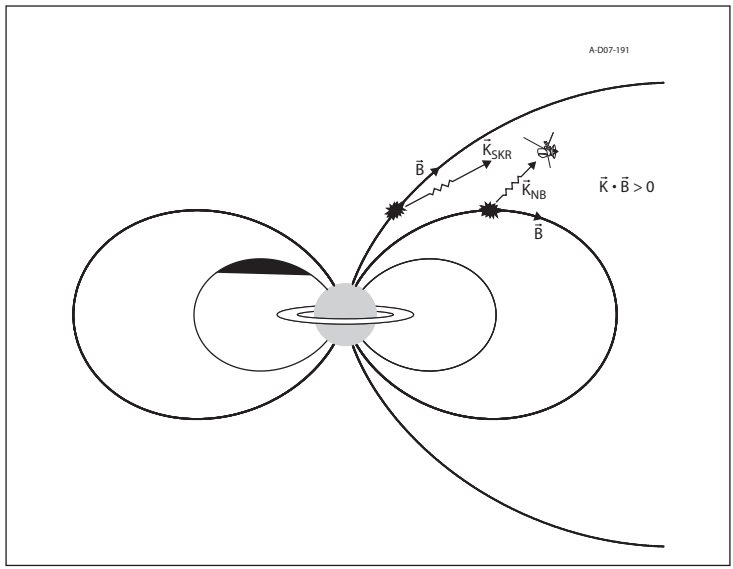

Figure 2: The geometry when Cassini detects both SKR and narrowband radio emissions in the northern hemisphere.

emissions, then the L–O mode fundamental could be generated by the wave–wave interaction between the electrostatic wave at f_{UH} and electrostatic waves at lower hybrid frequencies [Melrose, 1981; Barbosa, 1982], and the R–X mode second harmonic could be generated by a wave–wave interaction between two electrostatic waves at the upper hybrid frequency with opposite **k** vectors.

3.2 Source Location Indicated by Intensity Measurements

There have been several different conjectures on the source locations of narrowband emissions [Gurnett et al., 1981a; Louarn et al., 2007; Wang et al., 2010]. To resolve the uncertainty in the location of Saturn narrowband radio emissions, Ye et al. [2010a] followed the method Gallagher and Gurnett [1979] used to determine the time–averaged source location for auroral kilometric radiation (AKR) at Earth. In Figure 2 of Ye et al. [2010a], the averaged power flux of 5 kHz narrowband emissions detected by RPWS/HFR over 4 years is plotted versus the radial distance of Cassini. It is shown that as the radial distance R of Cassini increases, the power of the 5 kHz narrowband falls roughly as $1/R^2$ and the most intense emissions at 5 kHz are observed around 3 R_S. Color–coded trajectories of Cassini in the meridian plane for the five years from 2005 to 2009 (Figure 3 of Ye et al. [2010a]) showed that the most intense 5 kHz narrowband emissions are observed interior to the plasma torus.

4 Direction Finding Results

In the 2–antenna direction inversion, assuming no linear polarization (i.e., $Q = 0$ and $U = 0$), one can retrieve the direction of arrival (θ and ϕ), Poynting flux S and the circular polarization V of the radio waves. This inversion has been used in the statistical study of SKR properties [Lamy et al., 2008] and the case study of SKR source locations [Cecconi et al., 2009]. The narrowband emissions have been found to be purely circularly polarized when observed at high latitudes but partially polarized or unpolarized at low latitudes with no linear component [Ye et al., 2010a], which justifies the use of the 2–antenna direction inversion at least at high latitudes. It has also been shown in Ye et al. [2009] that the results of the 3–antenna and the 2–antenna direction inversion methods are consistent with each other. The result from the 2–antenna/3–antenna direction inversion can be confirmed using a different direction finding technique based on the apparent polarization reversal. A 5 kHz narrowband emission observed during spacecraft rotations is selected for the comparison between the direction finding technique. In this event, the measured apparent circular polarization switches sign when the source crosses the antenna plane, which can be used to determine the source location.

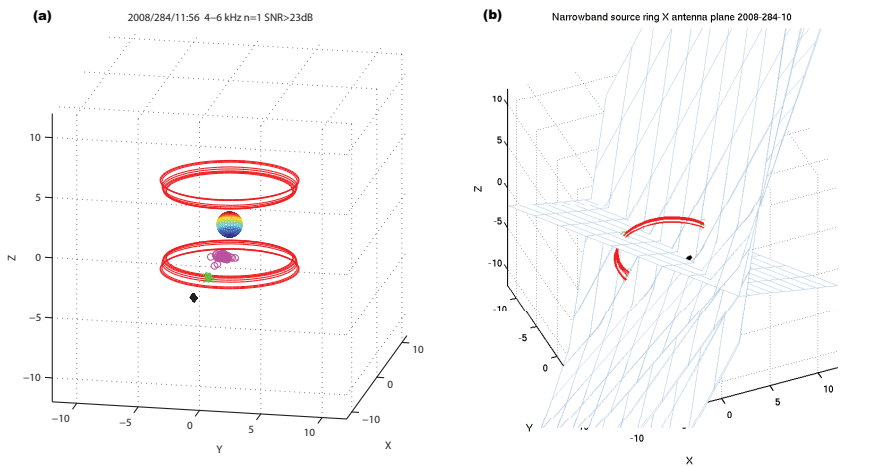

Figure 3: (a) 2–antenna direction finding result of the 5 kHz narrowband emission at 1100 SCET DOY 284, 2008; (b) direction finding based on two consecutive apparent circular polarization reversals.

Figure 3a shows the 2–antenna direction finding result of the 5 kHz narrowband emission at 1100 SCET DOY 284, 2008, assuming there is no linear polarization in the 5 kHz narrowband emission. In the 3D perspective of the source location, the spacecraft positions are represented by black diamonds. The red rings are the modeled source locations of the 5 kHz narrowband emissions based on the assumption that the narrowband emissions are mode converted from electrostatic upper hybrid waves on the outer boundary

of the plasma torus [Ye et al., 2009]. The locations of these rings are determined by the matching condition $f_{UH} = (n + 1/2)f_{ce}$, with $n = 1$. The multiple rings are due to the finite bandwidth (4–6 kHz) of 5 kHz narrowband emissions. There are multiple frequency channels of the HFR within this frequency range. Each ring corresponds to a modeled source location for a particular frequency channel. The purple circles are the interception points of the directions of arrival and the planes that contain the modeled source rings. The green dots are the interception points of the directions of arrival and the $f_{ce} = 5$ kHz surface. From this southern hemisphere perspective, the 5 kHz narrowband emissions appear to have a source in the auroral zone of Saturn rather than at the plasma torus as first suggested by Ye et al. [2009] and Wang et al. [2010].

The source of a radio emission is contained in the antenna plane when the apparent circular polarization reversal takes place. If there are two consecutive apparent polarization reversals and we assume the source location doesn't change within a short time, the direction of arrival can be determined by intersecting the two antenna planes at the time of apparent polarization reversals. The black dot in Figure 3b marks the location of the spacecraft. The antenna planes at the time of apparent circular polarization reversals are shown as well. The direction of arrival, which is the intersection line between the two planes, points to the polar region of Saturn and does not intersect the modeled ring. This is consistent with the 2–antenna direction finding result.

5 Z–mode Narrowband Emissions Below f_{ce}

In 2008, Cassini shifted to very high latitude (up to 75°) orbits. When the spacecraft was within a radial distance of 6 R_S, where $f_{ce} \geq 5$ kHz, intense narrowband emissions were observed below f_{ce}. In this underdense region, where f_{pe} is much lower than f_{ce}, f_{ce} is very close to f_{UH}.

Figure 4 (also Figure 5 from Ye et al. [2010a]) shows the wave electric field power and apparent polarization spectrograms of RPWS data from DOY 167/168, 2008. During the day, Cassini moved from high northern latitude to high southern latitude. The sudden switches in apparent circular polarization v_{app} of SKR from about 02:00 to 09:00 SCET on DOY 168 is caused by the source crossing the antenna plane during the spacecraft rotation. Between 13:00 and 14:00 SCET (marked by the closed dashed line), the 5 kHz narrowband emission crossed the local f_{ce}. The intensity of the 5 kHz narrowband emissions dropped by about 20 dB from below f_{ce} to above f_{ce}(upper panel). The apparent circular polarization of the 5 kHz narrowband emissions also switched from right hand (similar to SKR) below local f_{ce} to left hand (opposite to SKR) above local f_{ce} (middle panel). During the crossing of the 5 kHz iso–f_{ce} surface, the spacecraft was not rotating, so the apparent polarization reversal was not due to the radio source crossing the antenna plane. Rather, the change in polarization sense at local f_{ce} suggest a mode change from a right hand polarized mode to the L–O mode. Note also that the apparent total polarization degree of the 5 kHz narrowband emissions is < 1 below local f_{ce} and ~ 1 above local f_{ce} (lower panel).

Ye et al. [2010a] identified the right hand polarized 5 kHz narrowband emissions observed

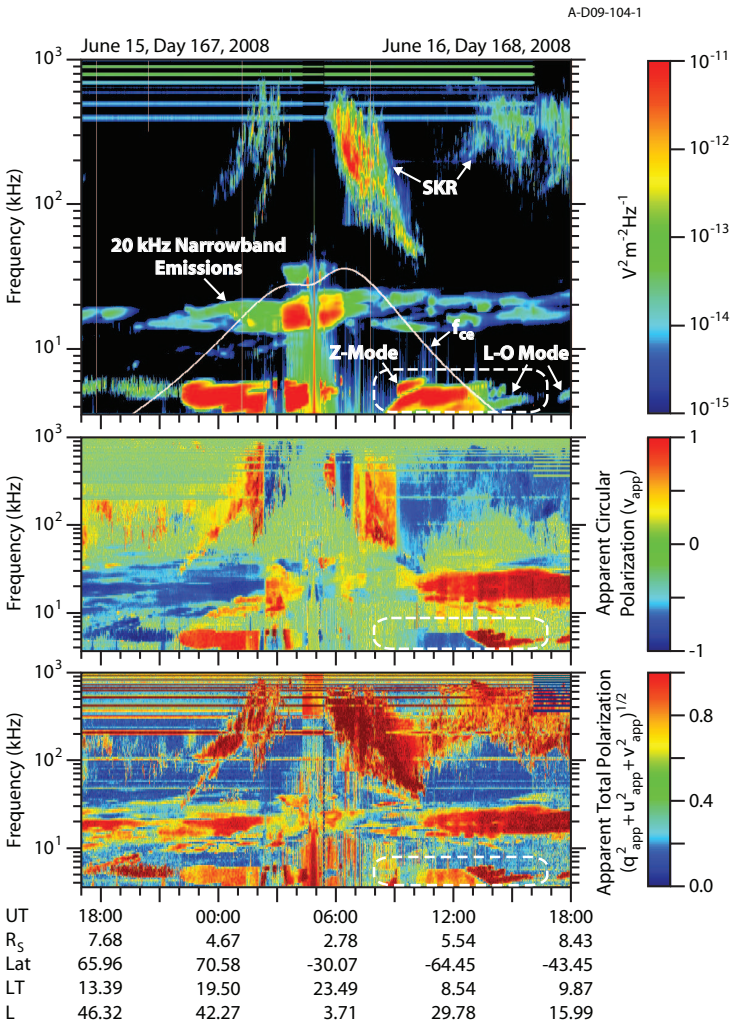

Figure 4: Wave electric field power and polarization spectrograms of Cassini RPWS on DOY 167/168, 2008. The upper panel shows the intensity, the middle panel the apparent circular polarization, and the lower panel displays the apparent total polarization.

below local f_{ce} as Z–mode waves. These Z–mode narrowband emissions can mode convert and escape as L–O mode narrowband emissions, which is normally observed above local f_{ce}. The dispersion relation diagrams from Sonwalkar et al. [2004] (their Figure 1) show the wave frequency as a function of the wave vector **k** as well as the polarization for different wave modes. In the underdense case ($f_{pe} < f_{ce}$), Z–mode is right hand polarized

between f_{pe} and f_{ce}. Between f_{pe} and f_{UH}, which is close to f_{ce}, both Z–mode and L–O mode narrowband emissions can exist. If the L–O mode narrowband emissions are mode converted from Z–mode waves, the intensity of the L–O mode would be much less than the Z–mode. Therefore, the polarization as measured by Cassini should be dominated by the Z–mode. The Z–mode wave is trapped below f_{UH}. So above $f_{UH} \sim f_{ce}$, only the L–O mode can exist. Below f_{ce}, the polarization of narrowband emissions is consistent with the Z–mode with total polarization degrees somewhat lower than 1. The low total polarization degree could result from multiple reflections of the waves due to trapping of Z–mode waves between the boundaries set by f_{UH} and $f_{L=0}$ surfaces.

In 2008, 21 events were observed where the circular polarization of the 5 kHz narrowband emissions switches sense and the intensity drops by about 20 dB as the spacecraft crosses the $f_{ce} = 5$ kHz surface. The times and locations of these events are listed in Table 1 of Ye et al. [2010a]. It is noticed that these events are mostly observed at relatively high latitudes and that the positions of Cassini at the time of the polarization reversals are around 6 R_S, practically the location of the $f_{ce} = 5$ kHz contour line at high latitude. 9 of Ye et al. [2010a]) shows a model of the possible region where the 5 kHz Z–mode narrowband emissions can propagate in the meridian plane, i.e. the region between the $f_{UH} = 4$ kHz and the $f_{L=0} = 6$ kHz contours. The Cassini trajectories where the 5 kHz Z–mode narrowband emissions were observed are well contained between the modeled boundaries since the Z–mode is a trapped mode.

6 Rotational Modulation

6.1 Clock–like Source

It has been shown that the intensity of SKR has a clock–like (or flashing light) modulation, which means SKR intensity reaches its maximum whenever a certain SKR longitude rotates to the subsolar point, independent of the location of Cassini with respect to Saturn [Warwick et al., 1981; Gurnett et al., 1981b]. In contrast, the modulation of the intensity of Saturn auroral hiss has been found to resemble a rotating beacon (or search light) [Gurnett et al., 2009b]. This indicates that auroral hiss is a beamed signal which is constantly on at a certain longitude. Therefore it is only observable when the spacecraft flies through the beam. Wang et al. [2010] showed that the 5 kHz Saturn narrowband emission has a clock–like source. This means that narrowband emissions are triggered periodically, possibly when a longitudinal anomaly rotates to certain local time of Saturn's magnetosphere. Additionally, narrowband emissions are not narrowly beamed so that they can be observed from a wide range of longitudes and local times.

To determine the modulation type and period of Saturn narrowband emissions, Ye et al. [2010b] employed a least–squares spectral analysis (also known as Lomb method) similar to what Gurnett et al. [2009a] developed to analyze the rotational modulation of SKR. Ye et al. [2010b] show that the modulation power of narrowband emissions has two peaks near the periods around 800 and 815 degrees/day based on the assumption of a clock–like source, whereas no obvious peaks are found for the rotating beacon source assumption.

This clearly confirms the result of Wang et al. [2010] that Saturn narrowband emissions have a clock–like source.

6.2 Indistinguishable Source Hemispheres

Ye et al. [2010b] investigated the existence of a possible north–south asymmetry in the rotational modulation period of Saturn narrowband emissions by creating two data sets, one for narrowband emissions observed at latitudes greater than 10°, and the other for latitudes less than -10°, similar to the way Gurnett et al. [2009a] differentiated the radiations from northern and southern sources of SKR. Unlike the case of SKR, where a north–south asymmetry was clearly revealed, the narrowband emissions display both modulation periods (800 and 815 degrees/day) in each hemisphere. Similar results are obtained for other data subsets with latitude limits of ± 20° or ± 30°.

Ye et al. [2010b] gave an explanation why 5 kHz narrowband emissions don't show a north–south asymmetry in their rotational modulation. Since Saturn narrowband emissions are mode converted from Z–mode waves that are trapped between propagation cutoffs at upper hybrid frequency f_{UH} and the cutoff frequency $f_{L=0}$, these electromagnetic Z–mode waves are refracted and guided by the cutoff surfaces as they propagate such that they can cross the equator either inside or outside the Enceladus plasma torus where the plasma density is low. At a density gradient or density irregularities, these Z–mode waves can mode convert to L–O mode and escape the trapping region. As a result, the modulated signals from both hemispheres can be observed in each hemisphere. On the other hand, the propagation of SKR and auroral hiss are relatively restricted to the same hemisphere they are generated in. So it is easier to isolate the emission from one hemisphere by restricting the latitude of observation.

6.3 Comparison to Saturn Kilometric Radiation Periods

Figure 5 (Figure 3 of Ye et al. [2010b]) shows a comparison of the rotational modulation rates of Saturn narrowband emission and SKR. The red dots represent the modulation rates of Saturn narrowband emissions which are obtained from the modulation spectrum analysis described above. For the time range when few narrowband emissions are observed, for example, from 2004 to 2006 and late 2007, the modulation rates are not determined, hence no red dots. The black dots represent the modulation rates of SKR given by Gurnett et al. [2009a]. The SKR periods are determined throughout the six years of study because SKR is observed continuously. Note that the second period of SKR, which is associated with the northern hemisphere of Saturn, only appears after the middle of 2006. This is because Cassini spent most of the time on the equatorial or slightly southern latitudes from 2004 to 2006, so the periodic signal of SKR from the northern hemisphere was not observed. During the time when Saturn narrowband emissions and SKR were both continuously observed, the modulation rates of Saturn narrowband emissions are nearly identical to those of SKR. There are exceptions though, when the red dots are more than 2 degrees/day off the black dots, for example the northern periods from late 2006 to early 2007 and early 2008. These gaps are still poorly understood.

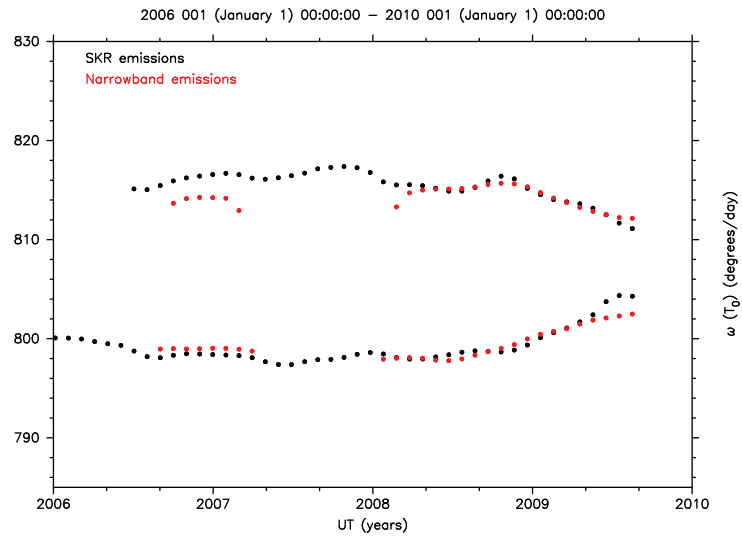

Figure 5: SKR vs. narrowband modulation periods from 2006 to 2010. The red dots represent the periods of Saturn narrowband emissions. The black dots represent the periods of SKR given by Gurnett et al. [2009a].

The fact that the 5 kHz narrowband emissions are modulated at two distinct rates which are identical to the SKR rates seems to support the argument that the 5 kHz narrowband emissions originate from the polar region. As discussed by Gurnett et al. [2009a] and Southwood and Kivelson [2009], the different rotation rates of northern and southern SKR could be explained by the magnetospheric slippage model, which mainly involves the transfer of angular momentum from the upper atmosphere to the magnetosphere. This momentum transfer is controlled by two factors: (1) the ionospheric conductivity; and (2) the high altitude zonal wind. Both of these two factors are dependent on the latitude as the incident angle of solar illumination would change with the latitude. As shown by Figure 5, the modulation rates of 5 kHz narrowband emissions show similar trend as SKR when the northern and southern rates are approaching each other. This suggests that the generation of the 5 kHz narrowband emissions are similarly affected by the rapid change of solar illumination angle on the auroral zones, which is most likely the source region of 5 kHz narrwoband emissions. However, as discussed in Ye et al. [2010b] there is a 90° phase lag between the 5 kHz narrowband emissions and SKR which seems to suggest they should be generated on different field lines.

7 Conclusion

The extended duration of the Cassini mission has allowed the RPWS instrument to capture narrowband emissions on thousands of occasions. The statistical and case studies

performed on these data gave many hints about the origins of this mysterious emission. (1) A new component of narrowband emissions was detected between 10 and 70 kHz in addition to the narrowband emissions originally detected by Voyagers around 5 kHz. This new component has its highest occurrence probability around 20 kHz. Source crossing events shown by Ye et al. [2009] indicates that the generation of these 20 kHz narrowband emissions is consistent with the mode conversion theory proposed by Gurnett et al. [1981a]. (2) Polarization measurements confirm that both 5 and 20 kHz narrowband emissions are propagating in the L–O mode, with the exception of some higher frequency narrowband emissions which are R–X mode second harmonic emissions generated by non–linear coupling of two electrostatic upper hybrid waves with opposite wave vectors. (3) No intense electrostatic upper hybrid wave is observed within the predicted source region of 5 kHz narrowband emissions by the mode conversion theory. Direction–finding results point to a source in the auroral zone rather than the plasma torus for the 5 kHz component. (4) Intensity measurements show that the 5 kHz narrowband emissions are most intense in the region between Saturn and the plasma torus, with the intensity peak around 3 R_S. One example of such intense narrowband emission is shown in Ye et al. [2010a], where the electric field spectral density of the emission is around $10^{-9}\mathrm{V}^2/\mathrm{m}^2\mathrm{Hz}$. The observed magnetic field spectral density for the same emission is around $10^{-8}\mathrm{nT}^2/\mathrm{Hz}$. The resulting cB/E ratio is close to 1, confirming the electromagnetic nature of narrowband emissions. (5) RPWS polarization measurements show that the intense narrowband emissions detected below the local electron cyclotron frequency (f_{ce}) are polarized as Z–mode. These Z–mode emissions are believed to be the source of the L–O mode narrowband emissions detected above the local f_{ce}. Although the energy source for the generation of the Z–mode waves is still unclear, linear growth rate calculations indicate that the observed plasma distributions are unstable to the growth of electrostatic cyclotron harmonic emission. Electromagnetic Z–mode could also be directly generated by the cyclotron maser instability [Menietti et al., 2009; Menietti et al., 2010]. (6) Similar to SKR, the 5 kHz NB emissions have a clock–like source and display two distinct modulation periods identical to the northern and southern hemisphere periods of SKR [Ye et al., 2010b]. This similarity supports the viewpoint that the 5 kHz narrowband emissions originate from the auroral zone. It has been shown by Ye et al. [2010a] that the Z–mode narrowband emissions observed below the local electron cyclotron frequency (f_{ce}) are the source of the 5 kHz narrowband emission. These Z–mode waves, upon reflection, propagate to the opposite hemisphere before escaping through mode conversion, which could explain the fact that both rotational modulation periods of 5 kHz narrowband emissions are observable in each hemisphere.

References

Ashour–Abdalla, M., and C. F. Kennel, Nonconvective and convective electron cyclotron harmonic instabilities, *J. Geophys. Res.*, **83**, 1531–1543, 1978.

Barbosa, D. D., Low–level VLF and LF radio emissions observed at Earth and Jupiter, *Rev. Geophys.*, **20**, 316, 1982.

Cecconi, B., and P. Zarka, Direction finding and antenna calibration through analytical inversion of radio measurements performed using a system of 2 or 3 electric dipole wire antennas on a three–axis stabilized spacecraft, *Radio Sci.*, **40**, RS3003, 2005.

Cecconi, B., L. Lamy, P. Zarka, R. Prangé, W. S. Kurth, and P. Louarn, Goniopolarimetric study of the revolution 29 perikrone using the Cassini Radio and Plasma Wave Science instrument high–frequency radio receiver, *J. Geophys. Res.*, **114**, A03215, 2009.

Fischer, G., B. Cecconi, L. Lamy, S.–Y. Ye, U. Taubenschuss, W. Macher, P. Zarka, W. S. Kurth, and D. A. Gurnett, Elliptical polarization of Saturn kilometric radiation observed from high latitudes, *J. Geophys. Res.*, **114**, A08216, 2009.

Gallagher, D. L., and D. A. Gurnett, Auroral kilometric radiation: Time averaged source position, *J. Geophys. Res.*, **84**, 6501, 1979.

Gurnett, D. A., W. S. Kurth, and F. L. Scarf, Narrowband electromagnetic emissions from Saturn's magnetosphere, *Nature*, **292**, 733–737, 1981a.

Gurnett, D. A., W. S. Kurth, F. L. Scarf, Plasma waves near Saturn: Initial results from Voyager 1, *Science*, **212**, 235–239, 1981b.

Gurnett, D. A., W. Calvert, R. L. Huff, D. Jones, and M. Sugiura, The polarization of escaping terrestrial continuum radiation, *J. Geophys. Res.*, **93**, 12,817–12,825, 1988.

Gurnett, D. A., et al. (29 co–authors), The Cassini Radio and Plasma Wave investigation, *Space Sci. Rev.*, **114**, 1, 395–463, 2004.

Gurnett, D. A., A. Lecacheux, W. S. Kurth, A. M. Persoon, J. B. Groene, L. Lamy, P. Zarka, and J. F. Carbary, Discovery of a north–south asymmetry in Saturn's radio rotation period, *Geophys. Res. Lett.*, **36**, L16102, 2009a.

Gurnett, D. A., A. M. Persoon, J. B. Groene, A. J. Kopf, G. B. Hospodarsky, and W. S. Kurth, A north–south difference in the rotation rate of auroral hiss at Saturn: Comparison to Saturn's kilometric radio emissions, *Geophys. Res. Lett.*, **36**, L21108, 2009b.

James, H. G., E. L. Hagg, and D. L. P. Strange, Narrowband radio noise in the ionosphere, *AGARD Conf. Proc.*, AGARD–CP–138, 24–1, 1974.

Jones, D., Source of terrestrial nonthermal radiation, *Nature*, **260**, 686–689, 1976.

Lamy, L., P. Zarka, B. Cecconi, R. Prangé, W. S. Kurth, and D. A. Gurnett, Saturn kilometric radiation: Average and statistical properties, *J. Geophys. Res.*, **113**, A07201, 2008.

Louarn, P., W. S. Kurth, D. A. Gurnett, G. B. Hospodarsky, A. M. Persoon, B. Cecconi, A. Lecacheux, P. Zarka, P. Canu, A. Roux, H. O. Rucker, W. M. Farrell, M. L. Kaiser, N. Andre, C. Harvey, and M. Blanc, Observation of similar radio signatures at Saturn and Jupiter: Implications for the magnetospheric dynamics, *Geophys. Res. Lett.*, **34**, L20113, 2007.

Melrose, D. B., A theory for the nonthermal radio continua in the terrestrial and Jovian magnetospheres, *J. Geophys. Res.*, **86**, 30, 1981.

Melrose, D. B., Emission at cyclotron harmonics due to coalescence of Z–mode waves, *Astrophys. J.*, **380**, 256–267, 1991.

Menietti, J. D., S.–Y. Ye, P. H. Yoon, O. Santolik, A. M. Rymer, D. A. Gurnett, and A. J. Coates, Analysis of narrowband emission observed in the Saturn magnetosphere, *J. Geophys. Res.*, **114**, A06206, 2009.

Menietti, J. D., P. H. Yoon, S.–Y. Ye, B. Cecconi, and A. M. Rymer, Source mechanism of Saturn narrowband emission, *Ann. Geophys.*, **28**, 1013–1021, 2010.

Rönnmark, K., H. Borg, P. J. Christiansen, M. P. Gough, and D. Jones, Banded electron cyclotron harmonic instability – a first comparison of theory and experiment, *Space Sci. Rev.*, **22**, 401, 1978.

Roux, A., and R. Pellat, Coherent generation of the auroral kilometric radiation by nonlinear beatings between electrostatic waves, *J. Geophys. Res.*, **84**, 5189, 1979.

Scarf, F. L., D. A. Gurnett, W. S. Kurth, and R. L. Poynter, Voyager–2 plasma wave observations at Saturn, *Science*, **215**, 587–594, 1982.

Sonwalkar, V. S., D. L. Carpenter, T. F. Bell, M. Spasojević, U. Inan, J. Li, X. Chen, A. Venkatasubramanian, J. Harikumar, R. F. Benson, W. W. L. Taylor, and B. W. Reinisch, Diagnostics of magnetospheric electron density and irregularities at altitude <5000 km using whistler and Z mode echoes from radio sounding on the IMAGE satellite, *J. Geophys. Res.*, **109**, A11212, 2004.

Southwood, D. J., and M. G. Kivelson, The source of Saturn's periodic radio emission, *J. Geophys. Res.*, **114**, A09201, 2009.

Wang, Z., D. A. Gurnett, G. Fischer, S.–Y. Ye, W. S. Kurth, D. G. Mitchell, J. S. Leisner, and C. T. Russell, Cassini observations of narrowband radio emissions in Saturn's magnetosphere, *J. Geophys. Res.*, **115**, A06213, 2010.

Warwick, J. W., J. B. Pearce, D. R. Evans, T. D. Carr, J. J. Schauble, J. K. Alexander, M. L. Kaiser, M. D. Desch, B. M. Pedersen, A. Lecacheux, G. Daigne, A. Boischot, and C. H. Barrow, Planetary Radio Astronomy observations from Voyager 1 near Saturn, *Science*, **212**, 239–243, 1981.

Willes, A., S. Bale, and Z. Kuncic, A Z mode electron–cyclotron maser model for bottomside ionosphere harmonic radio emissions, *J. Geophys. Res.*, **103**, 7017–7026, 1998.

Ye, S.–Y., D. A. Gurnett, G. Fischer, B. Cecconi, J. D. Menietti, W. S. Kurth, Z. Wang, G. B. Hospodarsky, P. Zarka, and A. Lecacheux, Source locations of narrowband radio emissions detected at Saturn, *J. Geophys. Res.*, **114**, A06219, 2009.

Ye, S.–Y., J. D. Menietti, G. Fischer, Z. Wang, B. Cecconi, D. A. Gurnett, and W. S. Kurth, Z mode waves as the source of Saturn narrowband radio emissions, *J. Geophys. Res.*, **115**, A08228, 2010a.

Ye, S.–Y., D. A. Gurnett, J. B. Groene, Z. Wang, and W. S. Kurth, Dual periodicities in the rotational modulation of Saturn narrowband emissions, *J. Geophys. Res.*, **115**, A12258, 2010b.